JOURNAL OF Applied Polymer SCIENCE

Graphene-Reinforced Biodegradable Poly(ethylene succinate) Nanocomposites Prepared by *In Situ* Polymerization

Jian Zhao, Xiaowei Wang, Weidong Zhou, Erjuan Zhi, Wei Zhang, Junhui Ji
Technical Institute of Physics and Chemistry, Chinese Academy of Sciences, University of Chinese Academy of Sciences, Beijing 100190, China
Correspondence to: J. Ji (E-mail: jhji@mail.ipc.ac.cn).

ABSTRACT: In this study, poly(ethylene succinate)(PES)/graphene nanocomposites were facilely prepared by *in situ* melt polycondensation of succinic acid and ethylene glycol in which contained well dispersed graphene oxide (GO). Fourier transform infrared (FTIR), GPC, TGA, and XRD were used to characterize the composites. The FTIR spectra and TGA measurement confirmed that PES chains had been successfully grafted onto GO sheets along with the thermal reduction of GO to graphene during the polymerization. GPC results indicated that increasing amounts of graphene caused a slight decrease in number average molecular weight of PES matrix when polymerization time was kept constant. The content of grafted PES chains on graphene sheets was also determined by TGA and was to be about 60%, which made the graphene sheets homogeneously dispersed in the PES matrix, as demonstrated by SEM and XRD investigations. Furthermore, the incorporation of thermally reduced graphene improved the thermal stability and mechanical properties of the composites significantly. With the addition of 0.5 wt % graphene, onset decomposition temperature of the composite was increased by 12°C, and a 45% improvement in tensile strength and 60% in elongation at break were also achieved. The enhanced performance of the composites is mainly attributed to the uniform dispersion of graphene in the polymer matrix and the improved interfacial interactions between both components. © 2013 Wiley Periodicals, Inc. J. Appl. Polym. Sci. 130: 3212–3220, 2013

KEYWORDS: poly(ethylene succinate); graphene; *in situ* polymerization; nanocomposites

Received 19 December 2012; accepted 15 May 2013; Published online 14 June 2013
DOI: 10.1002/app.39552

INTRODUCTION

In recent years, biodegradable polymeric materials have attracted a great deal of attention because of the serious environmental pollution problems caused by the commercial nondegradable plastics such as polypropylene (PP), polyethylene (PE), etc. Aliphatic polyesters are considered the most promising biodegradable materials. Poly(ethylene succinate) (PES), chemically synthesized through the polycondensation reaction of succinic acid (SA) and ethylene glycol (EG), is such an aliphatic polyester, which exhibits excellent melt processability and mechanical properties comparable to those of low-density polyethylene (LDPE).[1] However, as a potential commercial product for industrial applications, the thermal and mechanical properties of PES are often not sufficient. For example, the low melt viscosity and slow crystallization rate limit its application as film and injection molding products. Moreover, it is difficult to control the degradation performance of pure PES.[2] Blending with other biodegradable polymers and introduction of inorganic fillers are two effective ways to improve the properties of PES.[3–7] Lu et al.[5] investigated the crystallization and mechanical properties of PES/poly(L-lactide) (PES/PLLA) blends. The results showed that the isothermal crystallization mechanism of PES did not change in the blends, while the crystallization rate decreased with the increase of PLLA content. For the mechanical properties of the blends, elongation at break of PLLA was improved significantly and its considerably high Young's modulus was still kept. In another work, Suprakas and Mamookho[7] used organically modified montmorillonite (o-mmt) as fillers to prepare PES nanocomposites and investigated the thermal properties of the composites. It was showed that the incorporation of o-mmt stopped the super-cooling effect and accelerated crystal growth of PES matrix significantly and also improved the thermal stability of neat PES dramatically.

Graphene, a one-atom-thick plannar sheet of sp^2-bonded carbon atoms, has attracted tremendous attention in recent years due to its unique electronic, mechanical, and thermal properties.[8–12] It has been used to fabricate nanocomposites with high performance and novel functionalities for a range of potential applications such as electric conductive composites,[13–15] ultrasensitive sensors,[16] super-capacitor electrodes[17]and thermally stable, and mechanically reinforced materials.[18,19] However, the manufacture of such composites with optimized performance

requires not only the graphene sheets can be produced on a sufficient scale, but also they should be homogeneously dispersed in polymer matrices. Because of hydrophobic nature and high specific surface area, graphene sheets have a strong tendency to agglomerate, which severely restricts their promising applications. In contrast to graphene, graphene oxide (GO) sheets consist of covalently attached oxygen-containing groups, such as hydroxyl, epoxy, and carboxyl groups, which can alter the van der Waals interactions significantly and facilitate the dispersion of GO in solvent, as well as in the polymeric matrix.[20,21] More importantly, GO incorporated in the composites can be reduced into graphene to restore conjugated structure via a chemical or thermal method.[22–24] So, utilizing GO instead of graphene is a feasible way to prepare graphene-reinforced polymer composites. For example, Xu and Gao[25] prepared nylon-6/graphene composites by *in situ* ring-opening polymerization of caprolactam in the presence of GO. It was proved that GO was thermally reduced to graphene simultaneously and homogeneously dispersed in the nylon-6 matrix, revealing an excellent reinforcement effect to the composites.

In this study, we present a way to prepare the biodegradable PES/graphene nanocomposites by *in situ* melt polycondensation. First, GO sheets were exfoliated in EG with ultrasonic treatment to obtain a homogeneous dispersion state; then the polymer composites were prepared by polycondensation of SA and EG containing well dispersed GO under high temperature and high vacuum conditions. During the polymerization, PES chains were grafted onto GO sheets, accompanied by the thermal reduction of GO to graphene and homogeneous dispersion in final composites. As a result, the thermal stability and mechanical properties of the composites were all improved with low graphene loadings.

EXPERIMENTAL

Materials

Graphite powders were purchased from Qingdao Haida Graphite. Potassium permanganate ($KMnO_4$), sulfuric acid (H_2SO_4, 98%), hydrogen peroxide (H_2O_2), hydrochloric acid were purchased from Sinopharm Chemical Reagent (Shanghai, China). EG, SA, tetrabutyl titanate (TBT), and other reagents were purchased from Beijing Chemical Reagent Company (Beijing, China). All materials were used without further purification.

Preparation of PES/Graphene Nanocomposites

GO was synthesized from natural graphite powder by oxidation with $KMnO_4$ in concentrated H_2SO_4 according to the Hummers method.[26] Preparation of PES/graphene composites was performed in the following way. An appropriate amount of GO was first dispersed in EG (32.60 g, 0.525 mol) with the aid of vigorous agitation and ultrasonic treatment for 1 h to obtain homogeneous solution in a 250 mL three-neck round bottom flask. Then SA (59.05 g, 0.5 mol) and TBT (as a catalyst, 0.2 g) were added into the solution. The mixture was dehydrated at 180°C under nitrogen for 2 h with mechanical stirring until no more water was produced. Then the temperature was increased to 230°C, and the pressure was reduced to 60 Pa for condensation polymerization. The color of the mixture changed gradually from brown to black and the viscosity also increased during the reaction. After 5 h the reaction was stopped and the product was vacuum dried at 80°C for 24 h. According to the GO loadings, PES composites were labeled as PES/G-0.05, PES/G-0.1, PES/G-0.2, PES/G-0.5, which stood for the contents of GO being 0.05, 0.1, 0.2, and 0.5 wt %, respectively. Neat PES was synthesized under the same condition and used as a control.

Separation of PES-Grafted Graphene

To investigate the interactions between PES chains and graphene surface, the PES-grafted graphene was separated from the polymer matrix through a successive centrifugation/redissolution procedure[27,28] described as follows: 20 g composites were dissolved in 200 mL chloroform, then the suspension was centrifuged at 10,000 rpm for 30 min to make the graphene completely precipitated. Afterwards, the supernatant solution was poured into methanol (5 times in volume) to obtain free PES by precipitation; the solid material was dispersed in chloroform with ultrasonic treatment and stirred for 1 h before being separated by centrifugation again. This centrifugation and dissolution procedure was performed repeatedly for 5 times. To remove completely the physically absorbed PES from the graphene surface, the solid material was then extracted using chloroform in a Soxhlet extractor for 24 h. The finally obtained material, PES-grafted graphene, was dried at 80°C under vacuum and was labeled as PES-*g*-G.

Characterization

Atomic force microscopy (AFM) images of GO sheets were taken in the tapping mode on a Nano Scope IIIa Multimode apparatus (Veeco Instruments). The samples were prepared by spin-coating the solution onto freshly cleaved mica substrates at 1000 rpm. Fourier transform infrared (FTIR) spectra were recorded on an Excalibur 3100 spectrometer (KBr disk) and the spectra were collected between 500 and 4000 cm^{-1} with a spectral resolution of 4 cm^{-1}. The thermogravimetric analysis (TGA) was conducted on a TA Q50 instrument in a nitrogen atmosphere from ambient temperature to 600°C at a heating rate of 10°C/min. The flow rate of N_2 is 60 mL/min. About 5 mg sample was used for each test. GPC measurements were performed on Waters 2414 equipped with a differential refractive index detector at 35°C. $CHCl_3$ was used as eluent (1 mL/min). Molecular weight of the samples was calibrated according to polystyrene standards with a narrow molecular weight distribution. X-ray diffraction (XRD) patterns of the samples were recorded on Bruker D8 focus, using Cu-Ka radiation set at a voltage of 40 kV and a current of 40 mA. The differential scanning calorimetry (DSC) analysis was carried out on a Mettler–Toledo instrument under a constant nitrogen flow of 50 mL/min. Each sample was first heated to 150°C at a heating rate of 10°C/min, soaked for 5 min to erase previous thermal history, then cooled to −40°C at a cooling rate of 10°C/min, and heated to 150°C again at the same heating rate. Scanning electron microscopy (SEM) was performed on Hitachi S4800 scanning electron microscope with the acceleration voltage of 20 kV. Samples were prepared by immersing the molded bars in liquid nitrogen for 10 min before fracture. The fracture surfaces were previously coated with a conductive layer of gold before analysis. The mechanical properties were measured using an Instron instrument (Model 5966) in accordance with ISO

Applied Polymer SCIENCE

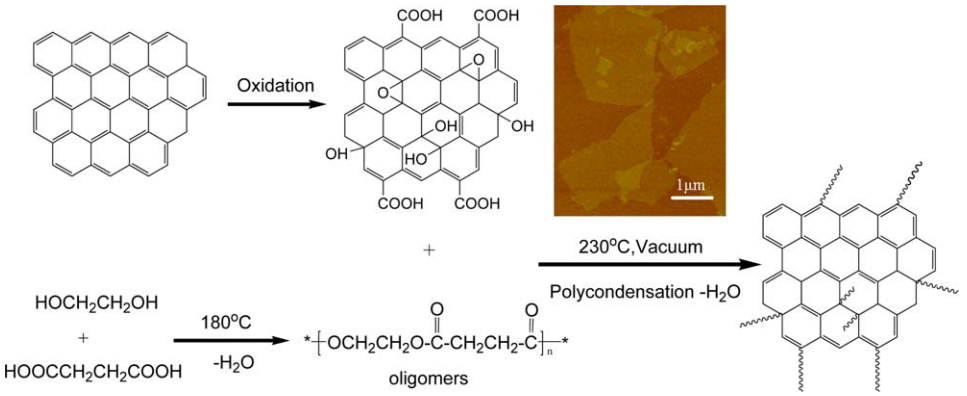

Figure 1. Illustration of the synthesis approach for PES/graphene composites. Insert AFM image shows the morphology of GO sheets dispersed in ethylene glycol. [Color figure can be viewed in the online issue, which is available at wileyonlinelibrary.com.]

527-2-2012 at room temperature. The speed of testing was 10 mm/min. Young's modulus was determined from the regression slope in the elastic region (0.05–0.25% strain) of the stress–strain curves. Polymer specimens were prepared into dumbbell-shaped bars with dimensions of 4 mm in width, 2 mm in thickness, 50 mm in length using a hot press machine, and then were annealed at room temperature for more than one week before measurements. Five tests were conducted for each sample, from which the mean values were obtained.

RESULTS AND DISCUSSION

Preparation of PES/Graphene Nanocomposites

In our experiments, PES/graphene composites with a range of graphene loadings were synthesized by *in situ* melt polymerization of SA and EG in the presence of GO, as presented in Figure 1. The pendent functional groups on GO platelets, such as carboxyl and hydroxyl groups, can offer strong interaction with the polar reaction monomer (EG), rendering a homogeneous dispersion of GO sheets in EG after sufficient ultrasonic treatment.[21] From the AFM image (Figure 1) it can be observed that the GO sheets were exfoliated well in EG and the dimension of GO sheets had about several hundred nanometers to several micrometers in length. The homogeneous dispersion of GO in EG prevented possible aggregation during melt polymerization and would result in homogeneous dispersion of graphene in the composites.

In the process of polycondensation, polymer chains of PES propagated through the esterification of EG and SA along with the consumption of monomers. Meanwhile, part of the PES chains were immobilized onto the GO sheets by condensation reactions between carboxyl (or hydroxyl) groups of GO and active hydroxyl (or carboxyl) groups at PES chains' terminals. At the later stage of reaction, high temperature and high vacuum were used, and the viscosity of the mixture increased gradually. For all samples, Weissenberg effect appeared at the end of the polymerization, indicating that PES with high molecular weight had been synthesized. Moreover, the color of the melting mixture turned from brown to black, suggesting the restoration of conjugated planes due to the thermal reduction of GO into graphene by decomposition of labile oxygen-containing moieties, such as epoxy and hydroxyl groups on GO.[25,29,30]

The weight average molecular weight (M_w), number average molecular weight (M_n), and the molecular weight distribution (PDI, equals to M_w/M_n) of pure PES and free PES collected from the supernatant of composites solution after centrifugation are listed in Table I. It can be observed that the addition of GO resulted in a slight decrease of number average molecular weight for the free polymers of the composites as compared to pure PES, also with a slight broader PDI from 2.1 to 2.2 or 2.3. The reason might be the grafting reaction of polymer chains onto the GO sheets during the melt polymerization because the active groups (mainly carboxylic acid groups) on GO sheets make GO act as chain terminators and disrupt the stoichiometric balance between carboxyl and hydroxyl groups in reaction system. Thus the higher content of GO means the more excessive carboxyl groups and the smaller molecular weight of polymer chains according to the condensation polymerization theory by Flory.[31] The reduction of molecular weight of the free polymers of the composites caused by grafting reaction between active groups on nanofillers with polymer chains was also found in *in situ* polymerized nanocomposites of PBS/TiO_2[32] and PBS/fumed silica.[33]

Characterization of PES-Grafted Graphene

To affirm the grafting polymerization of PES chains on graphene sheets, FTIR spectra of pure PES, GO, PES-grafted graphene isolated from composite of PES/G-0.5(labeled as PES-*g*-G/0.5), and thermally reduced GO (RGO, prepared by heating

Table I. Molecular Weight of Pure PES and Free PES of Composites Determined by GPC

Samples	M_n	M_w	PDI
PES	36,600	76,800	2.1
PES/G-0.05	35,700	78,500	2.2
PES/G-0.1	34,100	78,400	2.3
PES/G-0.2	33,200	73,000	2.2
PES/G-0.5	32,000	73,600	2.3

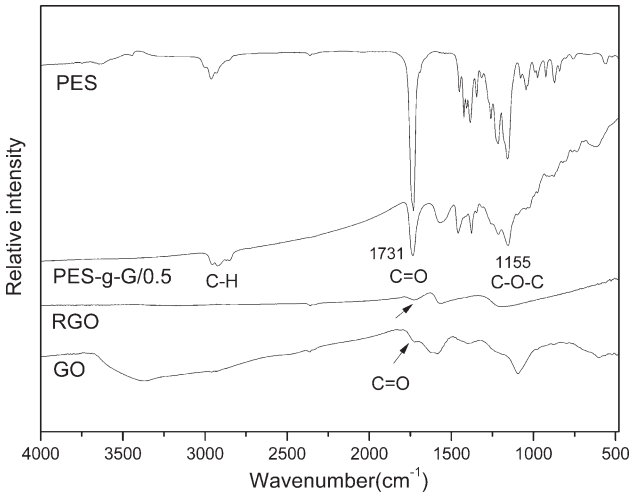

Figure 2. FTIR spectra of PES, GO, RGO, and PES-*g*-G/0.5.

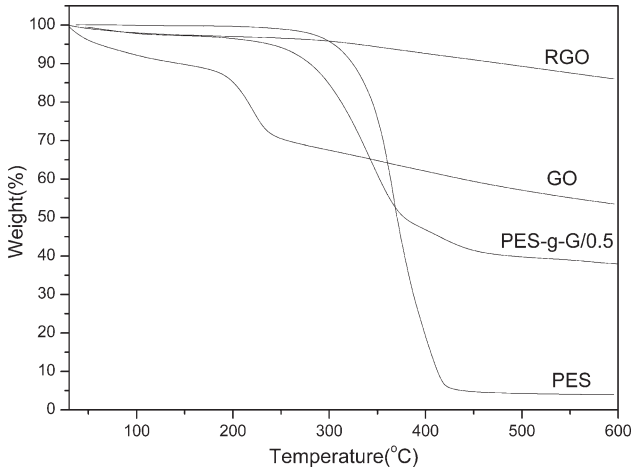

Figure 3. TGA curves of PES, GO, RGO, and PES-*g*-G/0.5.

neat GO under vacuum and at 230°C for 5 h, similar to the reaction condition) were recorded. As shown in Figure 2, PES showed strong C═O stretching vibration peak at 1731 cm^{-1}, C—O stretching vibration peaks at 1157, 1216 cm^{-1}, and C—H stretching vibration peaks at 2962 cm^{-1}. As for GO, characteristic bands appeared at 3370, 1723, 1583, 1095 cm^{-1}, attributed to the hydroxyl stretching vibrations of the C—OH groups, the C═O stretching vibrations of the —COOH groups, skeletal vibrations of unoxidized graphene domains, and C—O stretching vibrations of the carboxylic groups, respectively.[34,35] After heating treatment, the characteristic absorption bands of oxygen-containing groups decreased, indicating that GO had been reduced. Compared to the spectra of RGO, obviously increased absorption peaks of C═O (1731 cm^{-1}) and C—O—C (1155 cm^{-1}) stretching vibration appeared in the spectra of PES-*g*-G/0.5. These peaks came from the ester groups in PES main chains, meaning PES chains were still bonded on the graphene sheets even after at least 5 cycles of centrifugation/redissolution procedure and Soxhlet extraction for 24 h. The appearance of C—H stretching vibration peaks at 2850–2965 cm^{-1} also indicates the existence of polymer chains in the PES-*g*-G/0.5. All these results verify that some PES chains have been successfully grafted onto the GO sheets by esterification reaction along with the thermal reduction of GO during the polymerization.

The reduction of GO was further confirmed by TGA measurement. The weight loss curves of PES, GO, RGO, and PES-*g*-G/0.5 are presented in Figure 3. It is observed that the GO showed a very sharp weight loss within a narrow temperature range (200–250°C) because of the removal of oxygen-containing functional groups bonded to the GO sheets,[24] while such weight loss disappeared in the TGA curve of PES-*g*-G/0.5, similar to that of RGO, which indicates the amount of labile oxygen-containing groups on the GO sheets had a dramatic decrease during the melt polymerization. This decrease was caused by two reasons: the thermal decomposition of oxygen-containing groups and their grafting reactions with polymer chains. In contrast to pure PES, the PES-*g*-G/0.5 curve showed a 10 wt % weight loss below 300°C, revealing there were still some oxygenated functional groups bonded to the graphene sheets after thermal reduction and grafting reaction. It means that GO sheets were not thermally reduced to graphene completely during the melt polycondensation. The main weight loss of PES-*g*-G/0.5 took place at the temperature range of 300–400°C, which is slightly lower than that of the pure PES (about 320–400°C). This indicates that the grafted polymer chains were not so stable as the pure PES, which is due to the removal tendency of grafted PES on the graphene sheets and their relative lower molecular weight. On the basis of the weight loss of PES-grafted graphene below 550°C, the quantity of grafted PES on graphene sheets can be calculated and is to be about 60% in weight. From the discussion above, it can be concluded that the GO sheets had been thermally reduced to graphene simultaneously with sufficient grafting of PES chains during *in situ* polymerization.

Thermal Properties of the Composites

To understand the effect of graphene incorporation on the crystallization behavior of the PES matrix, DSC experiments of pure PES and composite samples were carried out according to the method described in experimental section. The thermograms were obtained from the second heating scan after erasing

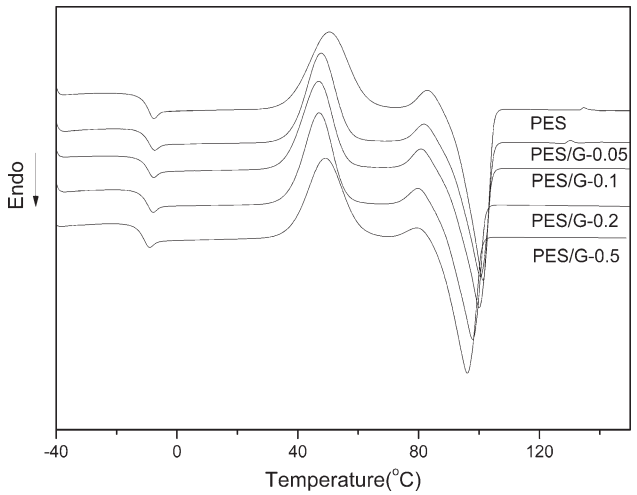

Figure 4. DSC thermograms of PES and its composites.

Applied Polymer SCIENCE

Table II. Thermal Properties of PES and Its Composites Determined by DSC

Samples	T_g (°C)	T_{cc} (°C)	ΔH_c (J/g)	T_m (°C)	ΔH_m (J/g)	χ_c (%)
PES	−10.6	50.5	51.8	101.0	55.2	30.7
PES/G-0.05	−10.5	47.6	48.2	100.2	53.0	29.4
PES/G-0.1	−10.6	47.0	48.3	99.7	53.1	29.5
PES/G-0.2	−10.5	46.9	47.9	97.7	51.2	28.5
PES/G-0.5	−10.3	48.9	49.2	96.9	50.4	28.1

thermal history, and presented in Figure 4. The glass transition temperature (T_g), cold crystallization temperature (T_{cc}), melting temperature (T_m), heat of melting (ΔH_m), heat of crystallization (ΔH_c), and crystallinity (χ_c) are summarized in Table II. Because of the slow crystallization rate of PES, no hot crystallization peaks were observed during the cooling process for all samples. This indicates when the cooling rate from melt was 10°C/min, it was very difficult for the PES matrix to crystallize and the sample stayed in a super-cooled state.[36] During the second heating scan, PES showed a broad cold-crystallization exothermic peak from 30 up to 70°C, which was accompanied by a second small exothermic peak due to the recrystallization. In the case of the composite samples, the cold-crystallization peaks became sharper and the temperature (T_{cc}) decreased with the increased graphene content. This is due to the nucleating role of the well dispersed graphene and the crystals of PES matrix grew faster than pure PES. But the nucleation effect was reduced when the graphene content increased up to 0.2 wt %. This implies that too many PES-grafted graphene sheets might not increase the number of crystalline nuclei further but might restrain the heterogeneous nucleation during the crystallization.[37] On the other hand, the well-dispersed graphene sheets blocked off the interconnected matrices to form confined regions of PES chains in the composites. The higher loading of graphene means the more confined mobility of polymer chains, which will lead to the formation of the incomplete crystals with lower thermal stability during the crystallization. Thus, the T_m values of the composites showed a regular decrease with increasing graphene content. Another reason for such phenomenon is that the molecular weight of the polymer matrix decreased with increasing GO content during polymerization mentioned earlier.[38] Moreover, the depressed crystallization caused by the introduction of graphene led to a decrease of χ_c ($\chi_c = \Delta H_m / [(1-\varphi)]\Delta H_0) \times 100\%$, where $\Delta H_0 = 180$ J/g,[39] φ is the weight fraction of the filler) from 30.7% for pure PES to 28.1% for PES/G-0.5, as shown in Table II.

The thermal stability of pure PES and its composites was investigated by TGA under an inert nitrogen atmosphere. The thermograms are shown in Figure 5, and the decomposition data are summarized in Table III. These data available from the TGA traces include: $T_{0.05}$, the temperature at which 5% degradation occurs, which is considered as the onset temperature of degradation; $T_{0.5}$, the temperature at which 50% degradation occurs, which is another measurement of thermal stability; and finally, the residue at 550°C, the nonvolatile fraction at 550°C.

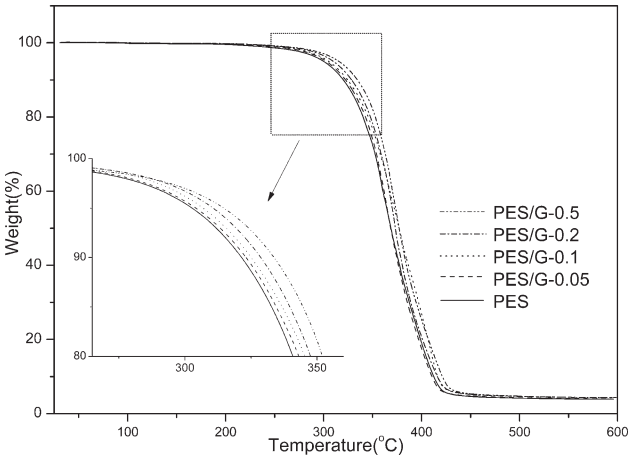

Figure 5. TGA curves of PES and its composites.

Graphene is a material with excellent thermal stability, which can improve the thermal properties of polymer composites. In this study, thermally reduced graphene with grafting of PES chains was introduced into the composites. As shown in the TGA thermograms, decomposition curves of the composites shifted towards the higher temperature region when compared to that of pure PES, indicating the composites showed higher thermal stability than pure PES. As for the composite of PES/G-0.5, its $T_{0.05}$ was about 12°C higher than that of pure PES. This pronounced improvement is attributed to the presence of well dispersed graphene in the polymer matrix. Since thermal degradation of polymers begins with chain cleavage and radical formation, the graphene in the composite may act as radical scavengers and hence delay the onset of thermal degradation. These results are in accordance with many other graphene-based polymer composites, which also showed improved onset thermal stability.[40,41] During the main thermal degradation process, the so-called "tortuous path" effect of graphene slowed the diffusion of the volatile degradation products and retarded the escape of these products out of the composites, leading to the improvement of thermal properties.[42] It should be noted that the value of $T_{0.5}$ did not increase regularly with the variation of the graphene content. It may be attributed to the increasing amount of grafted macromolecules with lower molecular weight and lower thermal stability than the free linear polymer chains. Furthermore, the residual weight percentages above 550°C were increased for the composites as compared to that of pure PES, suggesting the presence of graphene in the composites. This

Table III. Decomposition Data of PES and Its Composites Determined by TGA

Samples	$T_{0.05}$ (°C)	$T_{0.5}$ (°C)	Residue at 550°C (%)
PES	302.7	368.6	3.2
PES/G-0.05	304.1	368.5	3.6
PES/G-0.1	306.9	377.2	4.2
PES/G-0.2	310.2	373.6	4.3
PES/G-0.5	314.6	377.3	4.6

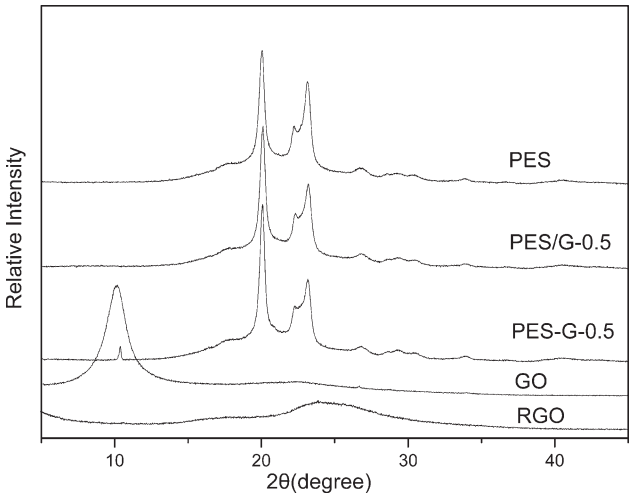

Figure 6. XRD patterns of GO, RGO, PES, and its composites.

increasing tendency corresponds to the variation of GO's loadings during the *in situ* polymerization.

Graphene Dispersion and Its Enforcement Effect to the Composites

Because of the strong π–π stacking between layers and incompatible surface characteristics with the polymer matrices, graphene sheets are prone to aggregate in the composites. So it is usually difficult to manufacture composites with well-dispersed graphene using common method such as melt blending.[43] The *in situ* polymerization technique can solve this problem. In this study, the key point of this approach is to disperse the GO sheets into the reaction monomer (EG) homogeneously with the assistance of effective ultrasonic treatment before polymerization. Figure 6 shows the XRD patterns of GO powders, RGO sheets, pure PES, and two composite samples: one is PES/G-0.5, prepared from EG with well dispersed GO sheets; the other is labeled as PES-G-0.5, containing the same weight percentage of graphene but was prepared from the EG in which GO was not dispersed with ultrasonic treatment, meaning that GO sheets were exfoliated incompletely in EG. On the basis of this, it is interesting to observe that a new small diffraction peak at 2θ value of 10.3° appeared in the XRD pattern of PES-G-0.5, which is very close to that of the characteristic peak of GO powders (2θ value, 9.6°). This indicates that there was still a small amount of GO sheets with stacking structure in the PES-G-0.5 sample even after thermal reduction during polymerization. As for the PES/G-0.5, the homogeneous dispersion of GO sheets in EG prevented their possible aggregation and ensured the uniform dispersion of graphene in the final composite. Therefore, such peak was not observed. Moreover, the RGO sheets exhibited a broad diffraction peak around 24°, due to the certain degree of restoration of π–π stacking structure after thermal reduction. This peak was not observed in the XRD patterns of all the composite samples. It is resulted from the successful grafting of PES chains onto graphene, which prevented the aggregation of graphene sheets during polymerization. The homogeneous dispersion of grafting-functionalized graphene sheets in composites was also revealed by SEM investigation of the fracture surfaces of pure PES and its composites. As shown in Figure 7, in contrast to the smooth surfaces of PES, much rougher surfaces were observed on the fracture surface of composites with the increased graphene content. These stretched and wrapped patterns were caused by the flake-like morphology

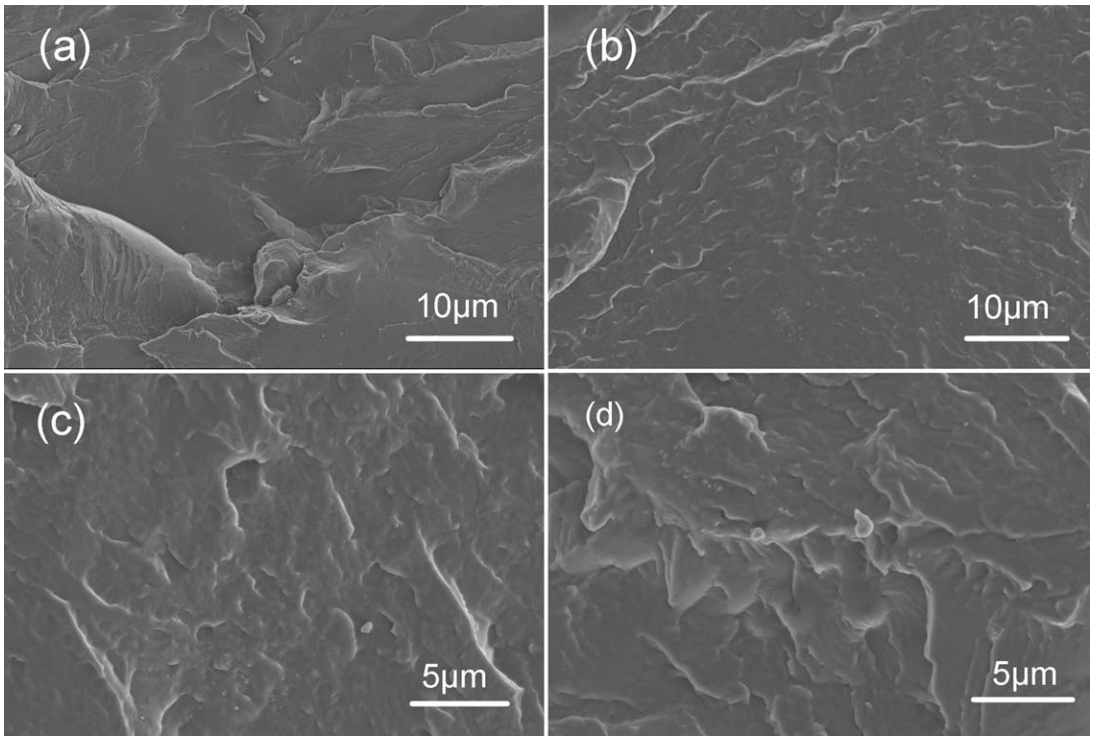

Figure 7. SEM images of the fracture surfaces of PES and its composites: (a) PES; (b) PES/G-0.1; (c)PES/G-0.2; and (d) PES/G-0.5.

Applied Polymer SCIENCE

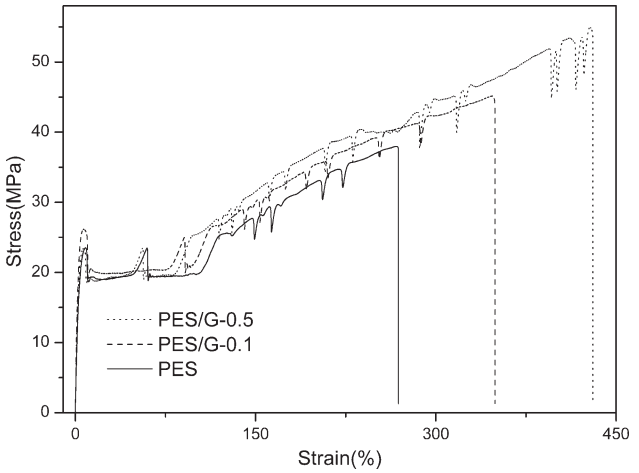

Figure 8. Stress–strain curves of PES and its composites with 0.1 and 0.5 wt % graphene.

of graphene sheets which had been embedded into the polymer matrix. Strong adhesion between graphene sheets and PES matrix ensured the uniform distribution of graphene in the host polymer. In short, the homogeneous dispersion of graphene is ascribed to the high grafting density, which enhances the interfacial interactions between the matrix and the graphene; it is also attributed to the *in situ* polymerization approach, in which graphene sheets are kept homogeneously dispersed during the reaction process.

Because of the outstanding mechanical properties, graphene sheets have been applied to reinforce composites in the previous research.[42,44] On the basis of the aforementioned investigations, the homogeneous dispersion of graphene sheets in PES matrix would result in the potential reinforcement to the composites. The stress–strain curves of pure PES and its composites are depicted in Figure 8. Relationships between tensile strength and Young's modulus with graphene content are shown in Figure 9. To distinguish statistical differences ($P < 0.05$) between PES/G composites and pure PES (as control), a one-factor analysis of variance (ANOVA) was performed on the data of mechanical properties.[45] Results are represented in Table IV. It is showed that the pure PES revealed a typical yield behavior with

Table IV. Mechanical Properties of PES and Its Composites from the Tensile Test

Samples	Tensile strength (MPa)	Elongation at break (%)	Young's modulus (MPa)
PES	38.4 ± 0.9^a	268 ± 20^a	380 ± 15^a
PES/G-0.05	42.4 ± 1.2^b	325 ± 21^b	411 ± 21^b
PES/G-0.1	44.2 ± 0.7^c	350 ± 16^c	485 ± 17^c
PES/G-0.2	47.4 ± 0.8^d	405 ± 14^d	430 ± 20^d
PES/G-0.5	54.1 ± 1.0^e	428 ± 19^e	410 ± 18^b

The superscript letters (a–e) represent the ANOVA results. The same letter denotes that the difference between two treatments is not statistically significant. Otherwise, the difference is statistically significant.

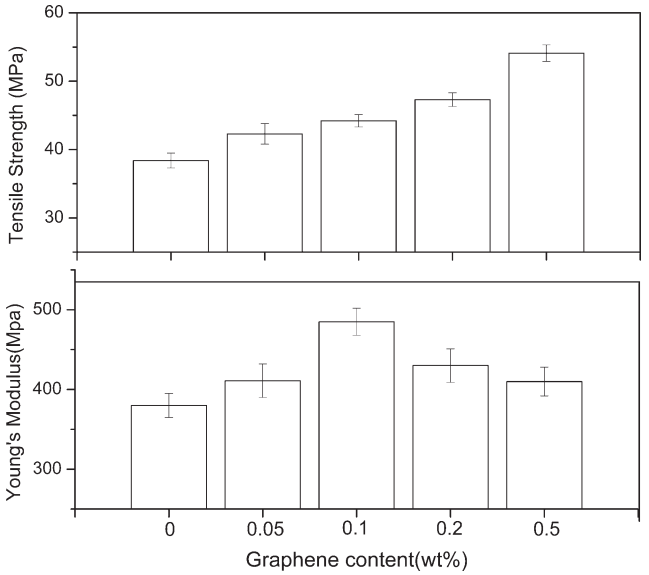

Figure 9. Variation of tensile strength and Young's modulus with the graphene content.

increasing stress during tension and the corresponding tensile strength and elongation at break were 38 MPa and 268%, respectively. Along with the increasing loading of graphene, the tensile strength and elongation at break of the composites were all improved. When the graphene content increased to 0.5 wt %, the tensile strength was dramatically enhanced to 54 MPa, which was higher than that of pure PES by 45%. More importantly, it was accompanied by a 60% increase in elongation at break. This result is different from many other graphene-based polymer composites,[18,19] which showed a decrease in elongation at break when tensile strength increased. This makes it possible to prepare composites with high ultimate tensile strength as well as relatively high toughness and ductility. Figure 10 shows the magnification of initial part of stress–strain curves to calculate Young's modulus. It can be seen a significant increase in Young's modulus was obtained with the addition of graphene

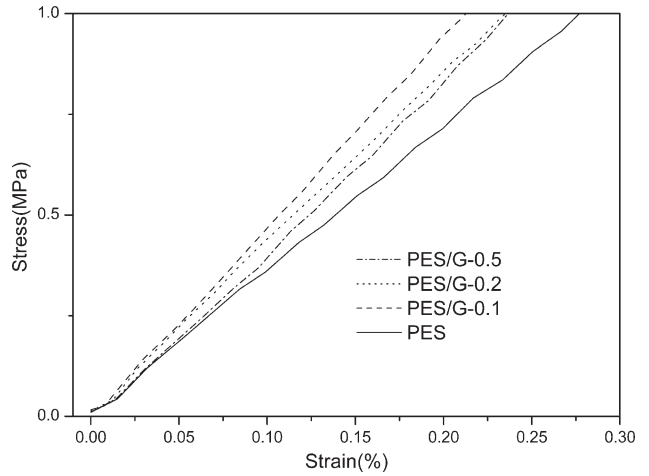

Figure 10. Magnification of the initial part of stress–strain curves to calculate Young's modulus.

lower than 0.1 wt %. This indicates an effective stress transfer between the interface of PES matrix and graphene, which benefits from the improved interfacial interactions by grafting of PES chains onto graphene surfaces. However, the Young's modulus showed a decrease trend when the graphene contents were higher than 0.2 wt %. This might be caused by the enhanced mobility of the grafted polymer chains on the graphene surfaces at higher graphene loadings. Another reason may be the decrease of crystallinity of the composites with increasing graphene contents.[46] Nevertheless, it should be noted that all the composite samples had higher modulus than pure PES. Obviously, the simultaneous improvements in strength, stiffness, and toughness of the composites are attributed to the good dispersion of graphene sheets in the composites and the improved interaction between the PES-grafted graphene and PES matrix. As discussed above, this profits from the implementation of *in situ* polymerization method.

CONCLUSIONS

In this work, PES/graphene composites were prepared by *in situ* polycondensation of related monomers in the presence of GO. The well dispersed GO in EG before polymerization resulted in the homogeneous dispersion of thermally reduced graphene sheets in the final composites. During the process of melt polymerization, the polymer chains were effectively grafted onto graphene sheets by the condensation reaction between the carboxyl (hydroxyl) groups on GO and active terminal ends of PES chains. As a result, the interfacial interaction between graphene sheets and PES matrix is significantly enhanced. It was showed that the PES/graphene composites exhibited an improvement in the thermal stability. Greatly improved mechanical properties including high strength and ductility haven also been achieved by introducing graphene sheets into pure PES, which will expand the industrial applications of the biodegradable PES. Furthermore, the *in situ* polymerization strategy verifies the validity to fabricate graphene reinforced polymer composites and provides a great promise for more extensive application of such composites.

ACKNOWLEDGMENTS

The authors gratefully acknowledge the financial supports provided by National Natural Science Foundation of China (No.30870620, 51003114). Thanks are expressed for the help of Dr. Mianqi Xue in the measurement of AFM.

REFERENCES

1. Fujimaki, T. *Polym. Degrad. Stab.* **1998**, *59*, 209.
2. Yoko, T.; Nariaki, I.; Kenichi, K.; Hiroshi, M. *Polym. Degrad. Stab.* **2004**, *84*, 115.
3. Yang, Y.; Qiu, Z. B. *J. Appl. Polym. Sci.* **2011**, *122*, 105.
4. Qiu, Z. B.; Ikehara, T.; Nishi, T. *Macromolecules* **2002**, *35*, 8251.
5. Lu, J. M.; Qiu, Z. B.; Yang, W. *Polymer* **2007**, *48*, 4196.
6. Zeng, J. B.; Zhu, Q. Y.; Li, Y. D.; Qiu, Z. C.; Wang, Y. Z. *J. Phys. Chem. B* **2010**, *114*, 14827.
7. Suprakas, S. R.; Mamookho E. M. *Polymer* **2009**, *50*, 4635.
8. Geim, A. K.; Novoselov, K. S. *Nat. Mater.* **2007**, *6*, 183.
9. Lee, C. G.; Wei, X. D.; Kysar, J. W.; Hone, J. *Science* **2008**, *321*, 385.
10. Du, X.; Skachko, I.; Barker, A.; Andrei, E. Y. *Nat. Nanotechnol.* **2008**, *3*, 491.
11. Li, X. S.; Zhu, Y. W.; Cai, W. W.; Borysiak, M.; Han, B.; Chen, D.; Piner, R. D.; Colombo, L.; Ruoff, R. S. *Nano. Lett.* **2009**, *9*, 4359.
12. Balandin, A. A.; Ghosh, S.; Bao, W. Z.; Calizo, I.; Teweldebrhan, D.; Miao, F.; Lau, C. N. *Nano. Lett.* **2008**, *8*, 902.
13. Eda, G.; Chhowalla, M. *Nano. Lett.* **2009**, *9*, 814.
14. Ansari, S.; Giannelis, E. P. *J. Polym. Sci. Part B: Polym. Phys.* **2009**, *47*, 888.
15. Zhang, H. B.; Zheng, W. G.; Yan, Q.; Yang, Y.; Wang, J. W.; Lu, Z. H.; Ji, G. Y.; Yu, Z. Z. *Polymer* **2010**, *51*, 1191.
16. Li, J.; Guo, S. J.; Zhai, Y. M.; Wang, E. K. *Anal. Chim. Acta* **2009**, *649*, 196.
17. Zhang, L. L.; Zhou, R.; Zhao, X. S. *J. Mater. Chem.* **2010**, *20*, 5983.
18. Liang, J. L.; Huang, Y.; Zhang, L.; Wang, Y.; Ma, Y. F.; Guo, T. Y.; Chen, Y. S. *Adv. Funct. Mater.* **2009**, *19*, 2297.
19. Fang, M.; Wang, K. G.; Lu, H. B.; Yang, Y. L.; Nutt, S. *J. Mater. Chem.* **2009**, *19*, 7098.
20. Stankovich, S.; Piner, R. D.; Nguyen, S. B. T.; Ruoff, R. S. *Carbon* **2006**, *44*, 3342.
21. Paredes, J. I.; Villar-Rodil, S.; Martinez-Alonso, A.; Tascón, J. M. D. *Langmuir* **2008**, *24*, 10560.
22. Stankovich, S.; Piner, R. D.; Chen, X. Q.; Wu, N. Q.; Nguyen, S. T.; Ruoff, R. S. *J. Mater. Chem.* **2006**, *16*, 155.
23. Stankovich, S.; Dikin, D. A.; Piner, R. D.; Kohlhaas, K. A.; Kleinhammes, A.; Jia, Y. Y.; Wu, Y.; Nguyen, S. T.; Ruoff, R. S. *Carbon* **2007**, *45*, 1558.
24. Wang, Z. L.; Xu, D.; Huang, Y.; Wu, Z.; Wang, L. M.; Zhang, X. B. *Chem. Commun.* **2012**, *48*, 976.
25. Xu, Z.; Gao, C. *Macromolecules* **2010**, *43*, 6716.
26. Hummers, W. S., Jr.; Offeman, R. E. *J. Am. Chem. Soc.* **1958**, *80*, 1339.
27. Yao, X. Y.; Tian, X. Y.; Xie, D. H.; Zhang, X.; Zheng, K.; Xu, J.; Zhang, G. Z.; Cui, P. *Polymer* **2009**, *50*, 1251.
28. Li, Y. H.; Chen, C. H.; Li, J.; Sun, X. S. *Polymer* **2011**, *52*, 2367.
29. Villar-Rodil, S.; Paredes, J. I.; Martinez-Alonso, A.; Tascón J. M. D. *J. Mater. Chem.* **2009**, *19*, 3591.
30. Hu, H. T.; Wang, X. B.; Wang, J. C.; Wan, L.; Liu, F. M.; Zheng, H.; Chen, R.; Xu, C. H. *Chem. Phys. Lett.* **2010**, *484*, 247.
31. Flory, P. J. Principles of Polymer Chemistry; Cornell University Press: New York, **1953**; Chapter 4.
32. Vassilioua, A. A.; Chrissafisb, K.; Bikiaris, D. N. *Thermochim. Acta* **2009**, *495*, 120.

33. Vassiliou, A. A.; Bikiaris, D.; Mabrouk, K. E.; Kontopoulou, M. *J. Appl. Polym. Sci.* **2011**, *119*, 2010.

34. Jeong, H. K.; Lee, Y. P.; Jin, M. H.; Kim, E. S.; Bae, J. J.; Lee, Y. H. *Chem. Phys. Lett.* **2009**, *470*, 255.

35. Bourlinos, A. B.; Gournis, D.; Petridis, D.; Szabó, T.; Szeri, A.; Dékány, I. *Langmuir* **2003**, *19*, 6050.

36. Papageorgiou, G. Z.; Bikiaris, D. N.; Achilias, D. S. *Thermochim. Acta* **2007**, *457*, 41.

37. Zhu, P. P.; Ma, D. Z. *Eur. Polym. J.* **2000**, *36*, 2471.

38. Chrissafisa, K.; Paraskevopoulosa, K. M.; Bikiaris, D. N. *Thermochim. Acta* **2006**, *440*, 166.

39. Papageorgiou, G. Z.; Bikiaris, D. N. *Polymer* **2005**, *46*, 12081.

40. Liang, J. J.; Huang, Y.; Zhang, L.; Wang, Y.; Ma, Y. F.; Guo, T. Y.;Chen,Y. S. *Adv. Funct. Mater.* **2009**, *19*, 2297.

41. Fabbri, P.; Bassoli, E.; Bon, S. B.; Valentini, L. *Polymer* **2012**, *53*, 897.

42. Cao, Y.; Feng, J.; Wu, P. *Carbon* **2010**, *48*, 3834.

43. Kim, H.; Miura, Y.; Macosko, C. W. *Chem. Mater.* **2010**, *22*, 3441.

44. Wang, X.; Yang, H. Y.; Song, L.; Hu, Y.; Xing, W. Y.; Lu, H. D. *Compos. Sci. Technol.* **2011**, *72*, 1.

45. Jin, S.; Matuana, L. M. *J. Vinyl. Addit. Techn.* **2008**, *14*, 197.

46. Raghu, A. V.; Lee, Y. R.; Jeong, H. M.; Shin, C. M. *Macromol. Chem. Phys.* **2008**, *209*, 2487.